

# Thermal Conductivity, Heat Capacity, and Cross-Linking of Polyisoprene/Single-Wall Carbon Nanotube Composites under High Pressure

Bounphanh Tonpheng, Junchun Yu, and Ove Andersson\*

Department of Physics, Umeå University, 901 87 Umeå, Sweden

Received September 28, 2009; Revised Manuscript Received October 10, 2009

**ABSTRACT:** Polyisoprene (PI)/single-wall carbon nanotube (SWCNT) composites and pure PI have been cross-linked by high-pressure treatment to yield densified elastomeric states. Simultaneously, the SWCNT and cross-linked-induced changes of the thermal conductivity, heat capacity per unit volume, and glass transition were investigated by in situ measurements. The thermal conductivity of both the elastomeric and liquid PI improves  $\sim 120\%$  by the addition of 5 wt % SWCNT filler. The SWCNT filler (5 wt %) increases the glass-transition temperature of liquid PI by  $\sim 7$  K and that of the elastomeric state by as much as 12 K, which is due to a filler-induced increase in the cross-link density. Moreover, the 5 wt % filler yields a heat capacity decrease by  $\sim 30\%$  in both the glassy and liquid/elastomeric states, which indicates that SWCNTs cause a remarkably large reduction of both the vibrational and configurational heat capacity of PI. Finally, the consequences of high-pressure densification and the possibilities this provides to help elucidating the nature of the heat conduction in polymer/carbon nanotube composites are discussed.

## Introduction

Since the discovery of carbon nanotubes (CNTs) in 1991,<sup>1</sup> these have been an interesting subject for studies, both because of their potential use in material science, optics, and electronics and as a test bed for fundamental science.<sup>2,3</sup> CNTs have extraordinary mechanical, thermal, and electrical properties that originate from their structure. CNTs can be regarded as rolled-up graphite sheets with essentially  $sp^2$  hybridized carbon units, which are formed into cylinders with nanometer-sized diameters. There are two main types of tubes: single-wall carbon nanotubes (SWCNTs) and multiwall carbon nanotubes (MWCNTs). The SWCNTs are typically  $< 2$  nm in diameter, and each end is capped with half of a fullerene molecule.<sup>4</sup> The MWCNTs have an inner diameter that varies from 1 nm up to a few nanometers, and their outer ranges vary from 2 nm up to a few tens of nanometers depending on the number of layers.<sup>5</sup>

The thermal conductivity,  $\kappa$ , of SWCNTs has been investigated both theoretically<sup>6</sup> and experimentally.<sup>7,8</sup> A molecular dynamics simulation of an isolated SWCNT indicates that  $\kappa$  is  $\sim 6000 \text{ W m}^{-1} \text{ K}^{-1}$  at room temperature and considerably higher at lower temperatures.<sup>6</sup> Although bulk samples have much lower  $\kappa$  because of large thermal resistance between individual CNTs, the  $\kappa$  value of aligned SWCNT bundles can be  $> 200 \text{ W m}^{-1} \text{ K}^{-1}$ .<sup>8</sup> Because  $\kappa$  of pure polymers is typically in the range of 0.1 to  $0.6 \text{ W m}^{-1} \text{ K}^{-1}$  (e.g., that of polyisoprene (PI) is  $0.15 \text{ W m}^{-1} \text{ K}^{-1}$ ),<sup>9</sup> the high  $\kappa$  value of CNTs makes these interesting as advanced nanofillers for improving  $\kappa$  as well as mechanical and electrical properties. Therefore, CNTs have a strong potential to enhance polymer properties, but simply mixing CNTs with polymers has proven to be insufficient for great improvement. The relative importance of issues such as homogeneous CNT dispersion in the polymer, CNT orientations and aspect ratio, polymer morphology, CNT–polymer, and CNT–CNT interfacial interaction for best progress is far from established. The scientific challenge to understand these issues and find the best route to take advantage

of the CNT properties has prompted tremendous interest, and many recent studies show promising progress.

Haggenmueller et al.<sup>10</sup> have reported a 600% increase in  $\kappa$  by adding 20 vol % SWCNTs in high density polyethylene. Besides the significant increase in  $\kappa$ , the result is interesting because the increase is stronger than that predicted by a linear dependence on the SWCNT content, which suggests a percolation effect. Haggenmueller et al.<sup>10</sup> hypothesized that this was due to polyethylene lamellae, which nucleate better on CNTs, causing crystalline bridges between SWCNTs bundles. As a result of the higher  $\kappa$  of crystalline polyethylene, this could possibly result in a percolation effect and an improved effective  $\kappa$  through thermal conduction via individual CNTs or bundles in a network linked partly by crystalline polyethylene.

In this work, we improve  $\kappa$  of the polymer matrix by applying high pressure. High-pressure densification of amorphous polymers induces a relative increase in  $\kappa$  by typically three times the relative change in density,  $\rho$ ; that is,  $\Delta\kappa/\kappa \approx 3\Delta\rho/\rho$ .<sup>11</sup> Moreover, the distance between the CNTs decreases as the sample densifies. A pressure increase of 1 GPa decreases the volume by a few tenth percent for a polymer, for example,  $\sim 19\%$  for PI at 350 K.<sup>12</sup> That is, if the volume changes isotropically, then the interparticle distance decreases  $\sim 7\%$  for PI at 350 K. Both of these effects improve the heat transfer between the highly thermally conducting CNT fillers. Pressurization may also decrease the interfacial thermal resistance between CNTs and between CNTs and the polymer matrix. The isothermal density dependence of  $\kappa$  is therefore an important parameter for detecting possible percolation behavior in CNT polymer composites and, consequently, a key parameter for understanding the heat transport in CNT composites.

A further possibility to improve the CNT–CNT and CNT–polymer interfacial interaction is high-pressure cross-linking, which can be induced in unsaturated polymers such as PI. As previously shown,<sup>13</sup> isothermal pressurization to high pressure  $\sim 0.5$  GPa, followed by an isobaric temperature increase to  $\sim 500$  K and subsequent annealing, yields significantly cross-linked PI. We have thus proven it possible to change PI into a densified

\*Corresponding author. E-mail: ove.andersson@physics.umu.se.

elastomeric state purely by high-pressure treatment at elevated temperature.<sup>13</sup> Here we use a similar procedure for samples of well-dispersed SWCNTs in PI and synthesize densified elastomeric nanocomposites by high-pressure treatments.

In this study,  $\kappa$  of PI and PI–SWCNT (1 and 5 wt %) composites has been studied by high-pressure, in situ measurements using the transient hot-wire method. The method has a higher accuracy and reliability compared with some methods used to study  $\kappa$  of polymer CNT composites. In particular, the thermal resistance between probe and sample, which can provide an uncertainty in other methods (e.g., those based on differential scanning calorimetry (DSC)), is here eliminated by the use of high pressure.

## Experimental Section

**Materials.** SWCNTs were produced by the electric arc discharge technique with a carbonaceous purity of 70–90% and metal content in the range of 7–10 wt % (Carbon Solution). The SWCNTs, which were examined by transmission electron microscopy (Figure 1), have a stated bundle diameter of 4 to 5 nm, average diameter of 1.4 nm, and lengths ranging from 500 nm to 1.5  $\mu\text{m}$ . The sample of liquid *cis*-1,4-poly(isoprene) (98 mol % unsaturation) made from natural rubber, with a number-average relative molecular mass of 38 000, was supplied by Sigma-Aldrich.

**Preparation of the PI–SWCNTs Composites.** The PI–SWCNT composites were prepared by ultrasonic treatment of SWCNTs and PI in toluene. The SWCNTs were dispersed in toluene using a 130 W, 20 kHz ultrasonic processor (VCX130, Sonics & Materials) at room temperature. The timer of the ultrasonic processor was set for 1 h, with a repeated sequence of 20 s ON, using 75% of full power, followed by 10 s OFF. PI was mixed in toluene using a magnetic stirrer until it was uniformly dissolved, and then the solution was added to the SWCNT–toluene mixture. Subsequently, the ultrasonic treatment of the PI–SWCNT–toluene mixture was continued using 50% of full power. The timer was set for  $\sim 1.5$  h with a repeated sequence of 20 s ON, followed by 40 s OFF, which caused the toluene to evaporate, and the mixture became progressively more viscous. Finally, the high-viscosity mixture was continuously dried for several days under dynamic vacuum at 70 °C to remove the remaining toluene, which was monitored by occasional weighing of the samples.

**Experimental Method for High-Pressure in Situ Study of the Thermal Properties.** The thermal conductivity  $\kappa$  and heat capacity per unit volume  $\rho c_p$  of pure PI and the PI–SWCNT composites were measured by the transient hot-wire method.<sup>14</sup> The hot-wire sensor was 0.1 mm in diameter, 40 mm long nickel (Ni) wire, which was placed horizontally in a circular shape within a Teflon cell. The wire was heated by  $\sim 3.5$  K by a 1.4 s long pulse of approximately constant power, and the resulting temperature variation was monitored by determining the electrical resistance; that is, the Ni-wire acted as both the heater and the sensor for the temperature rise. We calculated the temperature rise of the wire by using the relation between its electric resistance and temperature. The analytical solution for the Ni-wire temperature rise was fitted to the data points, thereby yielding both  $\kappa$  and  $\rho c_p$  with inaccuracies of approximately  $\pm 2$  and  $\pm 5\%$ , respectively.

The Teflon cell was filled with pure PI or a solvent-free composite and sealed with a tight-fitting Teflon lid. The Teflon cell was fitted into a piston-cylinder vessel device of 1 GPa capacity and then transferred to a hydraulic press. The temperature of the sample was measured using an internal Chromel–Alumel thermocouple. It was made from a wire batch that had been previously calibrated with an inaccuracy of  $< 0.2$  K, against a commercial diode temperature sensor (10 mK inaccuracy). The pressure,  $p$ , was determined from load/area with an empirical correction for friction, which had been established

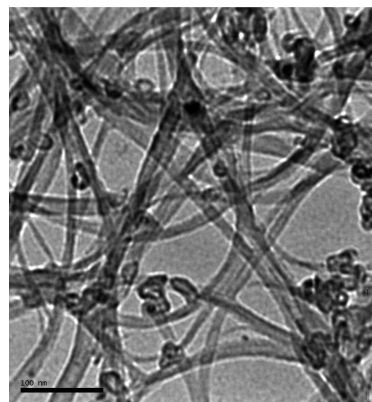


**Figure 1.** Transmission electron microscope image of the SWCNTs. The bar is 100 nm.

using the pressure dependence of a manganin wire. The pressure inaccuracy was estimated to be  $\pm 40$  MPa at 1 GPa. The temperature was controlled via an external electric coil heater for measurement above room temperature. The temperature and pressure were regulated using two independent PID-controllers. Using this procedure, the temperature could be kept to within  $\pm 0.5$  K during isothermal measurements, and the pressure to within  $\pm 1$  MPa during isobaric measurements. For measurements below room temperature, the vessel was cooled using liquid nitrogen.

**Characterization of Cross-Link Density after High-Pressure Treatment.** The cross-link density of PI and PI–SWCNT composites treated at 513 K and 1 GPa (0.8 GPa) was determined using the swelling method. The samples were swelled in *n*-heptane at room temperature until the swelling reached in equilibrium stage, which took about 48 h.

The cross-link densities were then calculated using the Flory–Rehner equation<sup>15,16</sup>

$$v = -[\ln(1 - \phi_{NP}) + \phi_{NP} + \chi\phi_{NP}^2]/[2V_s(\phi_{NP}^{1/3} - 2\phi_{NP}/f)] \quad (1)$$

where  $v$  is the cross-link density ( $\text{mol cm}^{-3}$ ),  $\phi_{NP}$  is the volume fraction of the network polymer in the swollen sample,  $V_s$  is the molar volume of the solvent (*n*-heptane,  $146.62 \text{ cm}^3 \text{ mol}^{-1}$ ),  $f$  is the functionality of the cross-linked network (here assumed to be a perfect tetrafunctional network, i.e.,  $f = 4$ ), and  $\chi$  is the polymer–solvent interaction parameter (natural rubber–heptane 0.5).<sup>17</sup> (Note that in refs 15 and 16,  $v$  is defined as the number of chains; therefore, for a tetrafunctional network, eq 1 differs by a factor of 1/2 from eq 12 given in ref 16.)

The volume fraction was calculated from

$$\phi_{NP} = ((m_d - m_f)/\rho)/\{((m_d - m_f)/\rho) + ((m_s - m_d)/\rho_s)\} \quad (2)$$

where  $m_d$  is the mass of the sample after swelling and subsequent drying,  $m_f$  is the mass of the filler in the sample,  $m_s$  is the mass of the swollen sample,  $\rho$  is the polymer density (PI  $0.92 \text{ g cm}^{-3}$ ), and  $\rho_s$  is the density of the solvent (heptane  $0.682 \text{ g cm}^{-3}$ ).

## Results and Discussion

**High-Pressure Cross-Linking at Elevated Temperature.** The thermal conductivity and heat capacity per unit volume,  $\rho c_p$ , of pure PI and PI–SWCNTs composites were studied both before and after treatment at 513 K and 1 GPa (5 wt % CNTs, labeled PI–SWCNT5 and pure PI) or 0.8 GPa (1 wt % CNTs, labeled PI–SWCNT1). This treatment induces significant cross-linking and transforms PI and the PI composites into elastomeric states, or network polymers. We have previously established that cross-linking of PI is insignificant

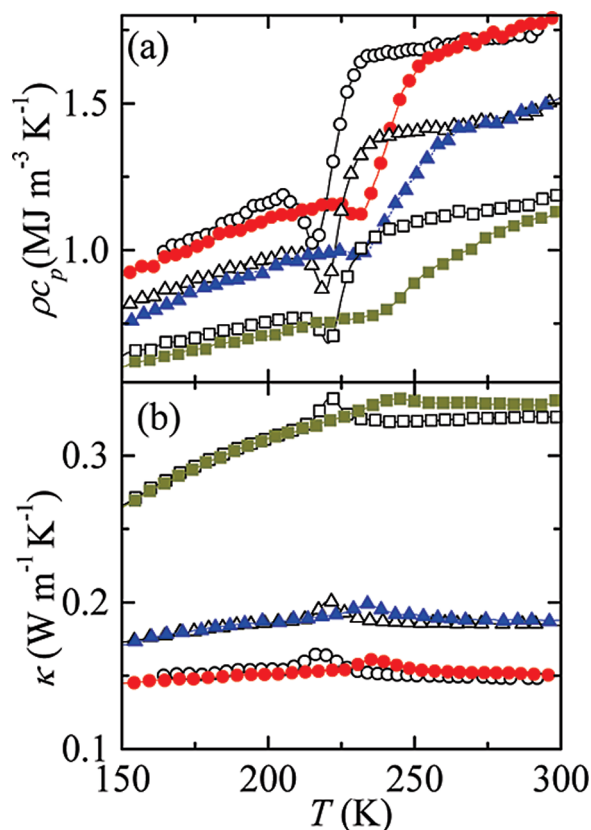


**Figure 2.** (a) Heat capacity per unit volume plotted against temperature on heating at 0.02 GPa for pure PI (○), cross-linked (●); PI-SWCNT1: (△), cross-linked (▲); and PI-SWCNT5: (□), cross-linked (■). (b) Simultaneously measured results for thermal conductivity.

below  $\sim 490$  K at 0.5 GPa.<sup>13,18</sup> To determine the properties of the samples without cross-links, we thus ensured that the temperature of the samples was always kept below  $\sim 450$  K. The temperature was thereafter raised to 513 K at 1 or 0.8 GPa and kept constant during 4 h to cross-link the samples. (The 4 h cross-link treatment at 0.8 GPa and 513 K for the PI-SWCNT1 sample was preceded by an identical treatment at 0.5 GPa; see ref 19.) The properties were simultaneously monitored as a function of time to study cross-linked induced changes in  $\kappa$  and  $\rho c_p$ , but no change was observed despite the fact that changes of  $\sim 1\%$  can be resolved. The cross-link densities of the samples were  $6.1 \times 10^{-4} \text{ mol cm}^{-3}$  for pure PI,  $1.2 \times 10^{-3} \text{ mol cm}^{-3}$  for PI-SWCNT5, and  $1.3 \times 10^{-4} \text{ mol cm}^{-3}$  for PI-SWCNT1, as subsequently determined by the swelling method. (See the Experimental Methods.) We can therefore conclude that a cross-link density of  $< 1.2 \times 10^{-3} \text{ mol cm}^{-3}$ , that is, the maximum value achieved here, does not induce changes in  $\kappa$  and  $\rho c_p$  by 1% or more at 1 GPa and 513 K. However, as described in more detail below, there is a significant cross-linked-induced change of the glass-transition temperature and changes in the thermal properties under conditions other than those for the cross-link process.

**Thermal Conductivity.** Figure 2b shows isobaric results for  $\kappa$  on heating at 0.02 GPa. The general behavior for all samples is similar to that of an amorphous state; that is,  $\kappa$  is almost constant or slightly increasing with increasing temperature. It is also possible to distinguish two temperature ranges with different  $d\kappa/dT$ , which are separated by the small peak in  $\kappa$ . (As discussed below, the peak in  $\kappa$  is associated with the glass transition in PI.) This is most apparent in PI-SWCNT5, as  $\kappa$  changes from moderately

increasing at temperatures below the peak to become almost temperature-independent above the peak. In pure PI, the change is less-pronounced, but  $d\kappa/dT$  changes from positive below the peak to negative above. The change in  $d\kappa/dT$  is due to the thermal expansivity increase at the glass-transition temperature,  $T_g$ , and the consequentially stronger decrease in density above  $T_g$  than below. The relative change of  $\kappa$  per degree ( $d(\ln \kappa)/dT$ ) decreases from  $2.4 \times 10^{-3}$  to  $2.5 \times 10^{-4} \text{ K}^{-1}$  for PI-SWCNT5, whereas the corresponding result for PI is  $1.7 \times 10^{-4}$  to  $-4.3 \times 10^{-4} \text{ K}^{-1}$ . The more than three times larger change for PI-SWCNT5 observed here is thus in agreement with the stronger enhancement of the thermal expansivity at  $T_g$  for CNT polymer composites than that for the pure polymer.<sup>20</sup>

At 0.02 GPa and 295 K,  $\kappa$  of PI-SWCNT5 is  $0.326 \text{ W m}^{-1} \text{K}^{-1}$ , and that for the cross-linked sample is  $0.334 \text{ W m}^{-1} \text{K}^{-1}$ . The corresponding value for PI-SWCNT1, which has been previously reported,<sup>19</sup> is  $0.185 \text{ W m}^{-1} \text{K}^{-1}$ , and slightly higher,  $0.187 \text{ W m}^{-1} \text{K}^{-1}$ , for the cross-linked sample. A similarly sized change occurs for pure PI when  $\kappa$  increases from 0.148 to  $0.151 \text{ W m}^{-1} \text{K}^{-1}$ . Therefore, although the cross-linking process does not affect  $\kappa$  at high pressure and elevated temperatures,  $\kappa$  consistently becomes a few percent higher at room temperature and atmospheric pressure. The cross-linked-induced changes for the samples are small but interesting from a fundamental point of view. We can identify three changes induced by the high-temperature, high-pressure treatment that can affect  $\kappa$ , that is, changes in (i) the number of covalent bonds between the chains, (ii) the density, and (iii) structural order. In a general case, these parameters could either decrease or increase with high-pressure, high-temperature treatments. For example, both chain scission and cross-linking can occur, and the density as well as the order can decrease or increase, for example, as a result of a decreased or increased degree of crystallinity. We have established that the sample becomes cross-linked, and there are no indications of significant chain scission. To establish roughly the pressure-induced change of density, we compared a pure PI sample cross-linked at 1 GPa (cross-link density  $6.1 \times 10^{-4} \text{ mol cm}^{-3}$ ) with pure PI cross-linked at 0.5 GPa (cross-link density  $2.7 \times 10^{-5} \text{ mol cm}^{-3}$ ) by simultaneously trying to submerge them in a suitable water-methanol mixture kept at  $25.0^\circ \text{C}$ . In a mixture of density  $0.949 \text{ g cm}^{-3}$  (29.9 wt % anhydrous methanol of 99.8% purity), none of the samples submerged. However, in a mixture of density  $0.940 \text{ g cm}^{-3}$  (34.8 wt % methanol), the 1 GPa treated sample submerged, whereas the 0.5 GPa sample only partially submerged. Because the stated density of virgin PI is  $0.92 \text{ g cm}^{-3}$ , this shows that the samples become progressively denser with increasing pressure of the high-temperature treatment. Concerning the structural order, that is, the third parameter iii, sulfidic cross-links and carbon-carbon cross-links tend to further decrease the already weak tendency of cold crystallization in PI.<sup>21</sup> A change of order would therefore be in the direction of decreased crystallinity, but because PI is difficult to crystallize, and the major part is inevitably amorphous, the difference is likely small. Moreover, a decreased crystallinity would also decrease  $\kappa$ . The increase in  $\kappa$  at room temperature and near atmospheric pressure is therefore attributable to the changes i and ii as an increased number of covalent bonds between the chains, and increased density would be beneficial for heat transport as well. A complementary view is that  $T_g$  increases because of cross-links, and thus the associated increase in the thermal expansivity shifts to higher temperatures. In the range between the  $T_g$  values of the samples, the larger expansivity of the untreated sample will



be unfavorable for its  $\kappa$  because  $\kappa$  decreases with decreasing density.

By the addition of 5 wt % (3.3 vol %) SWCNT,  $\kappa$  improves  $\sim 120\%$ , roughly independent of if the sample is in a viscous liquid state or cross-linked into a slightly densified elastomeric state. Therefore, the degree of cross-linking and the associated slight densification achieved here does not significantly improve the CNT–polymer phonon exchange. The large thermal resistivity that originates from the interfacial thermal resistance between PI and the CNTs and the low  $\kappa$  of the amorphous PI still governs the heat transport. This is particularly obvious from  $\kappa(T)$  as the temperature behavior of the composites has the same general behavior as that of pure PI. Moreover, as  $\kappa$  improves by about 25% by the addition 1 wt % CNTs, the increase in  $\kappa$  scales roughly linearly with CNT content.

For a theoretical estimate of  $\kappa$  for the composites, we use a model that can account for interfacial thermal resistance between the CNTs and the polymer. In this model,  $\kappa$  of a PI–SWCNT composite,  $\kappa_{\text{eff}}$ , is given by<sup>22</sup>

$$\frac{\kappa_{\text{eff}}}{\kappa_{\text{PI}}} = 1 + \frac{\phi p}{3} \frac{\kappa_{\text{SWCNT}}/\kappa_{\text{PI}}}{p + \frac{2a_k}{d} \frac{\kappa_{\text{SWCNT}}}{\kappa_{\text{PI}}}} \quad (3)$$

where  $p$  is the aspect ratio, that is, the ratio between the CNT length,  $L$  (1.5  $\mu\text{m}$ ), and the CNT diameter,  $d$  (1.4 nm),  $\kappa_{\text{SWCNT}}$  is the thermal conductivity of SWCNTs (6000  $\text{W m}^{-1} \text{K}^{-1}$  at room temperature),  $\phi$  is the volume fraction of CNTs, and  $a_k$  is a so-called Kapitza radius. It is defined by

$$a_k = R_k \kappa_{\text{PI}} \quad (4)$$

where  $R_k$  is the interfacial thermal resistance between the CNTs and PI. That is,  $R_k = 0$  corresponds to perfect thermal contact between the CNTs and the polymer.  $R_k$  has been estimated to be  $R_k \approx 8 \times 10^{-8} \text{ m}^2 \text{K W}^{-1}$ ,<sup>23</sup> and because  $\kappa_{\text{PI}} = 0.15 \text{ W m}^{-1} \text{K}^{-1}$ , this estimate yields  $a_k = 12 \text{ nm}$  for the PI–SWCNT composites.

At room temperature and atmospheric pressure, eq 3 yields  $\kappa_{\text{eff}} = 0.170 \text{ W m}^{-1} \text{K}^{-1}$  for PI–SWCNT1 and  $0.253 \text{ W m}^{-1} \text{K}^{-1}$  for PI–SWCNT5. These are somewhat lower than the experimental results of 0.185 and  $0.326 \text{ W m}^{-1} \text{K}^{-1}$  for PI–SWCNT1 and PI–SWCNT5, respectively. For a case without interfacial thermal resistance between the polymer matrix and the CNTs, that is,  $R_k = 0$ , eq 3 yields  $\kappa_{\text{eff}} = 13.4 \text{ W m}^{-1} \text{K}^{-1}$  for PI–SWCNT1 and  $66.2 \text{ W m}^{-1} \text{K}^{-1}$  for PI–SWCNT5. Considering the much too high predicted values by this simplification and other theories based on simple mixture rules, it is likely that the interfacial thermal resistance between the matrix and the CNTs strongly limits  $\kappa_{\text{eff}}$  of CNT composites,<sup>23</sup> but nonideal dispersion of the CNTs can also be a crucial factor. The interfacial thermal resistance arises from the constraints that the energy contained in high-frequency phonon modes, within the nanotubes, must be transferred to low-frequency modes through phonon–phonon coupling and vice versa. As discussed above,  $\kappa$  of CNTs is on the order of  $10^3 \text{ W m}^{-1} \text{K}^{-1}$ , and thermoplastics have  $\kappa$  in the range of  $0.1$  to  $0.6 \text{ W m}^{-1} \text{K}^{-1}$ ,<sup>9</sup> which gives a ratio  $\kappa_{\text{CNT}}/\kappa_{\text{polymer}} \approx 10^4$ . Although this ratio is large, it is significantly less than the corresponding ratio for electrical conductivity  $\sigma$ , which is  $\sigma_{\text{CNT}}/\sigma_{\text{polymer}} \approx 10^{15} - 10^{19}$ .<sup>24</sup> Therefore, the polymer will contribute to a larger fraction in thermal transport than in electrical conduction, which implies that different strategies must be employed for the best improvement of  $\kappa$  and  $\sigma$ , respectively. In the former case, crystalline domains around, and in between, CNTs, may significantly enhance  $\kappa$ , as indicated by the work of Haggemueller et al.<sup>10</sup>

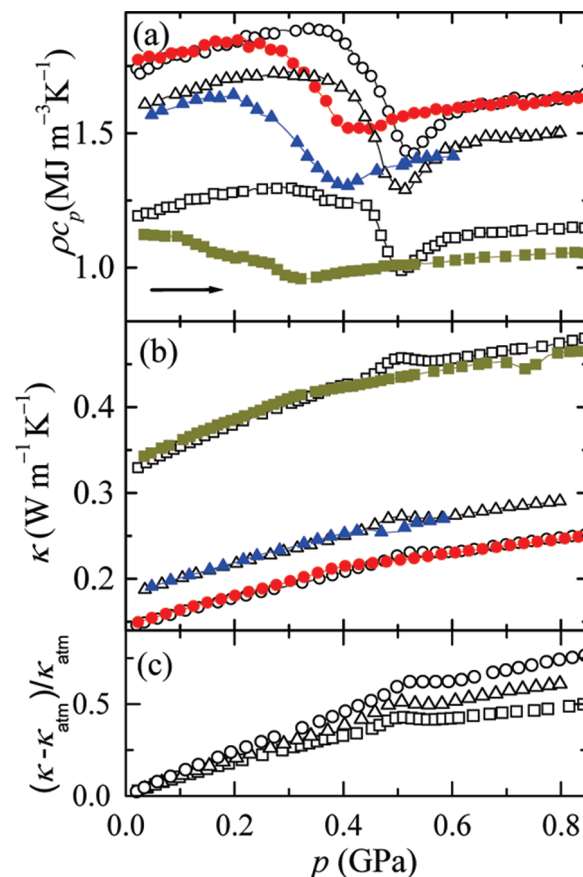


**Figure 3.** (a) Heat capacity per unit volume plotted against pressure on pressurization at 295 K for pure PI: (○), cross-linked (●); PI–SWCNT1: (Δ), cross-linked (▲); and PI–SWCNT5: (□), cross-linked (■). (b) Simultaneously measured results for thermal conductivity. (c) Fractional increase in thermal conductivity plotted against pressure for: pure PI (○), PI–SWCNT1 (Δ), and PI–SWCNT5 (□).

**Pressure and Density Dependence of the Thermal Conductivity.** The isothermal  $\kappa(p)$  behavior is similar for all samples, but the magnitudes differ depending on the CNT content (Figure 3b). These data also reveal the vitrification at isothermal pressurization. It occurs in the range of the anomalous peak in  $\kappa$  but is less apparent in the cross-linked samples. The vitrification reduces the increase in  $\kappa$  with increasing pressure, which is due to an increase in the bulk modulus at  $T_g$ . For two of the cross-linked samples, PI–SWCNT5 and PI–SWCNT1,  $\kappa(p)$  also exhibits a dip at  $\sim 0.75$  and  $0.5 \text{ GPa}$ , respectively. This was further studied by pressure cycles at high temperatures, and it moved to lower pressure with increasing temperature, which is a less common behavior for transitions. Moreover, no thermal effect was observed in the thermocouple signal. Although the dip can still be due to a transition, it can also be an experimental anomaly in the well-cross-linked sample. This feature requires further studies before the origin can be firmly established.

If the bulk modulus is known, then the isothermal density dependence of  $\kappa$ , as defined by the Bridgman parameter  $g = d(\ln \kappa)/d(\ln \rho)$ , can be calculated from the results of  $\kappa(p)$  shown in Figure 3b. The bulk modulus of CNT polymer composites have, however, rarely been studied and this is also the case for PI–SWCNT composites. For PI cross-linked at 1 GPa, we find  $g = 2.0$  using data for the isothermal bulk modulus,  $B_T$ , of vulcanized natural rubber ( $B_T = 1.95 \text{ GPa}$ ). This is in correspondence with our previous values for (liquid) PI ( $g = 2.2$ ) and PI cross-linked at

0.5 GPa and 513 K ( $g = 2.2$ ). Although the value for the composites cannot be calculated because of unknown  $B_T$ ,  $\kappa(p)$  provides valuable information concerning possible percolation behavior of  $\kappa$ . In the range up to 1 GPa at 295 K, the density of PI increases 15–20%,<sup>12</sup> and thus the inter-CNT distances decrease  $\sim 6\%$ . However, there is no indication here of percolation behavior, that is, that  $\kappa$  would start to increase stronger as a result of a well-conducting network consisting of SWCNTs. This is even more obvious in Figure 3c, which shows the fractional increase of  $\kappa(p)$ ,  $(\kappa - \kappa_{\text{atm}})/\kappa_{\text{atm}}$ , where  $\kappa_{\text{atm}}$  is the thermal conductivity at atmospheric pressure. It shows that the pressure-induced fractional increase is largest for pure PI.

It is important to note that this study of possible percolation behavior by pressure-induced densification is fundamentally different from those where the inter-CNT distance is instead decreased by increasing the amount of CNTs. With increasing CNT loading, the risk of agglomeration increases, which is not an issue in pressure densification. Moreover, the effect of pressure densification is manifold. Besides a decrease in the CNT–CNT distances,  $\kappa$  of the polymer improves, and the densification is normally also beneficial for the thermal contact between different constituent materials of a composite. In following studies, we will therefore investigate the possibility of realizing a highly thermally conducting network at higher pressures and with higher CNT content.

**Heat Capacity Per Unit Volume.** Figures 2a and 3a show the heat capacity per unit volume ( $\rho c_p$ ) as a function of temperature at 0.02 GPa and pressure at 295 K for PI and PI–SWCNT composites. The main changes of  $(\rho)c_p$ , shown in Figures 2a and 3a, occur in the vicinity of  $T_g$ , and are due to the arrests (cooling and pressurization) of the segmental and normal motions of PI, that is, the loss of the configurational part of  $c_p$ . (As explained further below, the dips in the data, for example, near 0.5 GPa at 295 K, are artifacts of the method because of the relaxation.) At temperatures below or pressures above the glass transition, the (skeletal) vibrational heat capacity provides the major contribution to  $c_p$ .<sup>25</sup> Outside the temperature and pressure ranges of the glass transition,  $\rho c_p$  increases on heating and pressurization, which are due to increases in  $c_p$  and  $\rho$ , respectively. As the sample is pressurized, the increase in the latter diminishes because of decreasing compressibility, and the increase in  $\rho c_p$  levels off.

By assuming that the heat capacities of PI and CNTs are additive, the values for the composites can be estimated using the mixture rule. The density  $\rho_C$  and specific heat capacity  $c_{p,C}$  of the composite are then given by

$$\rho_C = \frac{1}{\frac{w_{\text{PI}}}{\rho_{\text{PI}}} + \frac{w_{\text{CNT}}}{\rho_{\text{CNT}}}} \quad (5)$$

$$c_{p,C} = w_{\text{PI}}c_{p,\text{PI}} + w_{\text{CNT}}c_{p,\text{CNT}} \quad (6)$$

where  $w$  is the weight fraction. The density and specific heat capacity of SWCNT at room temperature and atmospheric pressure are  $\sim 1.5 \text{ g cm}^{-3}$  and  $600 \text{ J kg}^{-1} \text{ K}^{-1}$ ,<sup>26</sup> respectively. The corresponding values for PI are  $0.92 \text{ g cm}^{-3}$  and  $1900 \text{ J kg}^{-1} \text{ K}^{-1}$ . This yields a heat capacity per unit volume of 1.74 and  $1.72 \text{ MJ m}^{-3} \text{ K}^{-1}$  for PI–SWCNT1 and PI–SWCNT5, respectively, whereas the experimental values are 1.6 and  $1.2 \text{ MJ m}^{-3} \text{ K}^{-1}$ . Consequently, only a tiny fraction of the experimentally observed decreases of  $\rho c_p$  are due to the low  $c_p$  of CNTs. Therefore, the heat capacities of PI and SWCNT are not additive in the composite, which suggests that SWCNTs have a pronounced effect on the PI

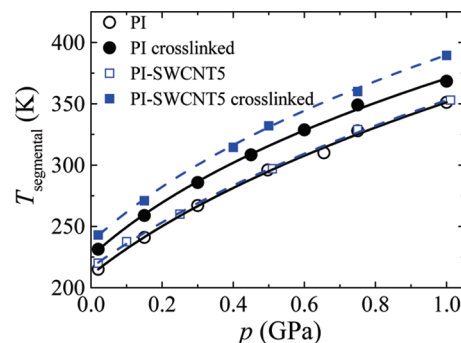


**Figure 4.** Arrest temperatures of the segmental modes, corresponding to a relaxation time of  $\sim 1$  s, plotted against pressure for PI and PI–SWCNT5. The dashed and solid lines represent fits of eq 7.

modes. With the density obtained from eq 5 and assuming that  $c_p$  of the CNTs is unaffected in the composite, the decreases in  $c_p$  for PI are 8 (PI–SWCNT1) and 31% (PI–SWCNT5). A detailed analysis of the results in Figures 2 and 3 shows that the absolute CNT-induced decrease in  $c_p$  is somewhat larger in the liquid state than in the glassy state, but the fractional decreases are identical in the two states to within the uncertainty. This indicates that the CNT-induced fractional reduction of the vibrational contribution to  $c_p$  is about the same as that for the configurational part, that is, that associated with the segmental and normal modes, at  $T_g$  ( $\sim 30\%$  when 5 wt % SWCNTs is added). However, because the vibrational  $c_p$  provides a larger contribution to the total  $c_p$ , it also accounts for the major part of the  $c_p$  decrease for PI above  $T_g$  and for the total  $c_p$  decrease for PI below  $T_g$ .

We turn to consider the heat capacity change due to cross-links, which is much less pronounced than the CNT-induced decrease. The results for PI–SWCNT5, with the highest cross-link density, show a slight  $\rho c_p$  decrease as compared with the sample before cross-linking. Moreover, as shown in Figure 2,  $\rho c_p$  decreases somewhat more in the elastomeric state at 295 K than in the glassy state, but again, the fractional change is about the same. In this case, however, the changes are too small to establish if the cross-links affect both the configurational and vibrational contributions, or primarily the latter. The decrease in  $\rho c_p$  is typically  $\sim 6\%$  in the elastomeric state. Therefore, because the density increase should be about the same as that for cross-linked PI at atmospheric pressure (2%),  $c_p$  decreases  $\sim 8\%$  as a result of the induced cross-link density of  $1.2 \times 10^{-3} \text{ mol cm}^{-3}$ .

**Glass-Transition Behavior.** In the vicinity of a glass transition, hot-wire results typically show a peak in  $\kappa$  and a dip in  $\rho c_p$ , which both are artificial anomalies, as well as an increase in  $\rho c_p$  on increasing temperature or decreasing pressure. Disregarding the dips in  $\rho c_p$ , the results in Figure 2a show the typical glass-transition characteristic of a sigmoidal increase in  $c_p$  on temperature increase. The peak and dip are associated with the onset of the segmental (and merged normal) modes and occur when the relaxation time for the modes becomes on the order of the probe time, that is, 1 s.<sup>27</sup> These arise because of the relaxation and the associated time dependence in  $c_p$  during the heating event, which is not accounted for because  $\kappa$  and  $\rho c_p$  are adjustable, time-independent parameters in the fitting of the analytical solution for the hot-wire temperature rise. (See the Experimental Section.) The characteristic features in  $\kappa$  and  $\rho c_p$  occur in a supercooled liquid state (ergodic state) in contrast with the nonergodic-to-ergodic state change during the sigmoidal  $c_p$  increase observed at  $T_g$  by normal DSC. The typical time-scale of DSC, which is set by the heating rate, is also longer

( $\sim 10^2$  s). We have here labeled the transition temperature, obtained from the dip in the isobaric  $\rho c_p$ ,  $T_{\text{segmental}}$ , to indicate these differences in time scale and characteristics and to specify that it is associated with the onsets of the segmental modes on heating. The values for the glass-transition temperature given here,  $T_{\text{segmental}}$ , are thus higher, typically  $\sim 10$  K, than those obtained by DSC using a heating rate of  $\sim 10$  K  $\text{min}^{-1}$ .

As shown in Figures 2 and 3, the glass-transition anomalies in  $\kappa$  and  $\rho c_p$  are shifted to higher temperatures, or lower pressures, for the samples cross-linked by the high-pressure treatment. The shift of  $T_{\text{segmental}}$ , as shown in Figure 4, is due to an increased rigidity of the polymer chains. It is most apparent for the PI-SWCNT5 sample, where the dip in  $\rho c_p$  shifts from  $\sim 0.5$  to  $\sim 0.3$  GPa at 295 K (Figure 3). Moreover, the glass-transition anomalies become less distinct and occur in wider pressure and temperature ranges after being cross-linked. The cross-linked-induced changes can be described by an increase in the average relaxation times and a wider distribution of relaxation times, which causes the increase in  $c_p$  to occur at higher temperatures and in wider temperature (pressure) ranges. In the isothermal data, it is also possible to distinguish a short plateau in the middle of the pressure range of the abruptly changing  $\rho c_p$ . This feature is also most pronounced in the PI-SWCNT5 sample and occurs at  $\sim 0.2$  GPa for cross-linked PI-SWCNT5. Therefore, the change of  $\rho c_p$ , which is associated with the glass transition, occurs in a two-step sequence, which is likely due to a slight difference in pressure for the onsets of the normal and segmental modes, where the latter occurs at higher pressures.

The values for  $T_{\text{segmental}}$ , taken from the dips in  $\rho c_p(T)$  and corresponding to a relaxation time of  $\sim 1$  s, are described well by the equation<sup>28</sup>

$$T_{\text{segmental}}(p) = T_0 \left( 1 + \frac{b}{a p} \right)^{1/b} \quad (7)$$

where  $a$ ,  $b$ , and  $T_0$  are fitting parameters and  $p$  is the pressure in GPa. The fits yielded  $T_0 = 236.92$  K,  $a = 0.85$  GPa, and  $b = 3.08$  for the cross-linked PI-SWCNT5 composite and  $T_0 = 216.44$  K,  $a = 1.04$  GPa, and  $b = 2.52$  for the untreated PI-SWCNT5 composite. In the case of cross-linked PI, the fit yielded  $T_0 = 225.43$  K,  $a = 0.83$  GPa, and  $b = 3.12$ . The values for untreated PI are  $T_0 = 209.4$  K,  $a = 0.81$  GPa, and  $b = 3.26$ , which has been previously reported.<sup>13</sup> From linear fits in the range up to 0.3 GPa, we obtain the initial pressure dependencies for the glass-transition temperature,  $(dT_{\text{segmental}}/dp)$ , to be 171 and 186 K  $\text{GPa}^{-1}$  for PI-SWCNT5 and cross-linked PI-SWCNT5, respectively. The corresponding data for PI and cross-linked PI are 185 and 194 K  $\text{GPa}^{-1}$ , respectively.

At atmospheric pressure,  $T_{\text{segmental}}$  increases  $\sim 7$  K by the addition of 5 wt % SWCNT. The corresponding result for 1 wt % SWCNT is  $\sim 3.5$  K,<sup>19</sup> which shows that  $T_g$  does increase with the addition of CNTs and that the initial increase with increasing CNT content is larger. Although  $T_g$  of a polymer has occasionally been found to be independent of or even decreasing with CNT content, an increase is most commonly observed. As one explanation for this behavior, it has been suggested that CNTs reduce the mobility of polymer chains locally in contact with CNTs,<sup>20,29</sup> and that this increases  $T_g$ . It has also been argued that this could give rise to a broader glass-transition range, that is, a wider temperature range for the sigmoidal increase in the heat capacity, as the sample would become heterogeneous on a small scale compared with the chain dimensions.<sup>29</sup> The results here show that CNTs reduce the polymer mobility so

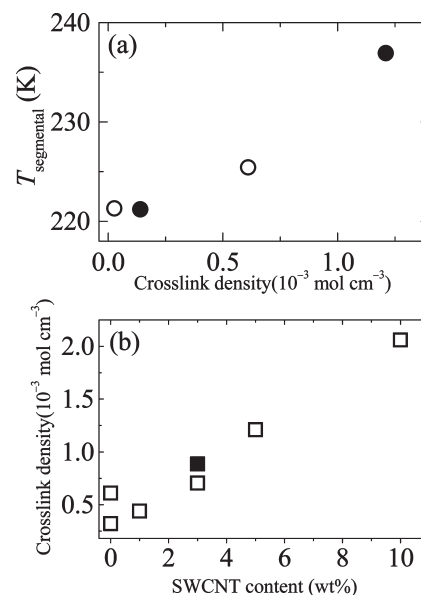


**Figure 5.** (a) Arrest temperatures of the segmental modes at atmospheric pressure, corresponding to a relaxation time of  $\sim 1$  s, plotted against cross-link density for PI (○) and PI-SWCNT (●). (The value for a cross-link density of  $2.7 \times 10^{-5} \text{ mol cm}^{-3}$  is taken from ref 13.) (b) Cross-link density plotted against carbon nanotube (□) and carbon black (■) content.

that the segmental motions become arrested at higher temperature on cooling. But a detailed analysis of the temperature range for the heat capacity increase shows that it is almost independent of CNT content for the untreated samples; that is, any change in the glass-transition range is too small to be resolved. The less-pronounced increase in  $T_g$  for a sample already containing CNTs would then mean that the CNT surface area is sufficient to reduce the mobility of essentially all chains already at low CNT content. Another possibility for an increasing  $T_g$  is a reduced free volume. That is, the addition of CNTs may decrease the available free volume and, thus, raise  $T_g$ . The leveling off of the  $T_g$  increase with increasing CNT content would be consistent with a more efficient initial filling of voids.

The cross-linking of PI-SWCNT5 causes  $T_{\text{segmental}}$  to increase as much as  $\sim 20.5$  K, which is more than the corresponding result for pure PI ( $\sim 16$  K). This means that the inclusion of 5 wt % CNTs in cross-linked PI appears to raise  $T_g$  by 11.5 K ( $7 + 4.5$  K), that is, 4.5 K more than for the same amount in untreated PI. Another significant difference between cross-linked PI and cross-linked PI-SWCNT5 composite is the broader glass transition for the latter. To assess the CNT influence on these effects of cross-linking, we first consider the change of  $T_{\text{segmental}}$  with cross-link density.

As shown in Figure 5a,  $T_{\text{segmental}}$  varies with the cross-link density for samples of both pure PI and PI-SWCNT composite. (The value for a cross-link density of  $2.7 \times 10^{-5} \text{ mol cm}^{-3}$  is taken from ref 13.) A linear extrapolation of the results for pure PI yields  $T_{\text{segmental}} = 230$  K at the cross-link density for PI-SWCNT5, which is 7 K lower than that observed, that is, the same difference as that between untreated PI and PI-SWCNT5. It follows that  $T_{\text{segmental}}$  is not increased more by the inclusion of CNTs in a cross-linked PI sample than in an untreated PI sample. The stronger increase of  $T_{\text{segmental}}$  for PI-SWCNT5 than for PI at cross-linking is instead due to an indirect effect of CNTs because the PI-SWCNT5 shows a higher cross-link density despite identical thermal treatment as for pure PI. To investigate



the influence of CNT/carbon filler on cross-link density in more detail, we produced four new composites and one pure PI by the same procedure as that for the other PI and PI–SWCNT5 samples. Three were PI–SWCNT composites with 1, 3, and 10 wt % CNTs, respectively, and one was PI with 3 wt % carbon black (N550). Although the samples were cross-linked by identical thermal treatments, they exhibited a trend of increasing cross-link density with increasing CNT/carbon content, as shown in Figure 5b. Because the swelling method used here to determine the cross-link density includes both chemical bonds and physical cross-links, this can be due to either CNT/carbon enhancement of the cross-linking efficiency or a CNT/carbon-induced increase in physical cross-links. The composite sample of PI with 3 wt % carbon black exhibited a cross-link density of  $8.8 \times 10^{-4}$  mol cm<sup>-3</sup>. This is in reasonable correspondence with a linear cross-link density dependence on carbon content (Figure 5b), which shows that the enhanced cross-link density for PI–SWCNT is not specific for carbon in the form of CNTs.

The results for  $\rho c_p$  show that the heat capacity step at  $T_g$  is narrower for the untreated samples than the corresponding cross-linked samples, that is, the glass-transition range increases with cross-link density. This effect of cross-linking has been previously discussed<sup>30</sup> and indicates a spatial heterogeneity for the environment of different cooperatively rearranging segments, or regions, in the terminology of Adam and Gibbs theory.<sup>31</sup> The structural constraints caused by the cross-links also limit the size of cooperatively rearranging regions, which yields a broad glass transition. The much broader glass transition in cross-linked PI–SWCNT5 than in cross-linked PI might, however, be increased by the presence of the CNTs. As shown in Figures 2 and 3, the cross-linked PI–SWCNT1 shows a slightly wider glass transition than cross-linked PI despite a lower cross-link density. Therefore, the results indicate that CNTs augment the broadening of the glass transition caused by the cross-links in the densified (cross-linked) samples.

## Conclusions

We conclude that the thermal conductivity of *cis*-1,4-polyisoprene (PI) with 5 wt % single-wall carbon nanotube (SWCNT) is ~120% higher than that of pure PI, and it increases roughly linearly with SWCNT content. Simultaneously, the heat capacity decreases by ~30% both below and above the glass-transition temperature, which indicates that the decrease is associated with a remarkably large reduction of both the vibrational and configurational heat capacity of PI. After treatment for 4 h at 513 K and 1 GPa, both PI and PI–SWCNT composites become cross-linked into densified elastomeric states, with only small changes in the thermal conductivity and heat capacity but significant increases in the glass-transition temperatures and the widths of the glass transitions. Despite identical thermal treatment to cross-link the samples, the glass-transition temperature increases more for PI with 5 wt % CNTs than for pure PI, which is due to a filler (carbon) induced enhancement of the cross-link density. The results also indicate that CNTs augment the broadening of the glass transition in the densified elastomeric states but not in the untreated samples.

Although the thermal conductivity does not significantly improve more for the PI–SWCNT composites synthesized here at 1 GPa pressure than that for composites made under atmospheric pressure conditions, we like to stress the improved possibilities high-pressure studies offer in nanocomposite research. In particular, pressure-induced densification decreases the interparticle (e.g., CNT–CNT) distances without the risk of

agglomeration and improves the thermal and electrical contact between the constituent materials of the composite. Moreover, for polymer/CNT composites, the effect of changing polymer properties can be studied with unaltered CNT spatial distribution. In this study, the effect of high-pressure cross-linking was established for PI, but for a semicrystalline polymer one may increase the degree of crystallinity by high-pressure treatment, which would strongly enhance the thermal conductivity of the matrix. Consequently, investigations at high pressures offer improved possibilities of realizing thermal as well as electrical percolation networks in polymer CNT composites and obtaining further insight into the nature of thermal and electric transport.

**Acknowledgment.** This work was financially supported by SIDA/SAREC of Sweden and the Swedish Research Council.

## References and Notes

- (1) Iijima, S. *Nature* **1991**, 354, 56–58.
- (2) *Carbon Nanotubes: synthesis, Structure, Properties, and Applications*; Dresselhaus, M. S.; Dresselhaus, G.; Avouris Ph., Eds.; Topics in Applied Physics 80; Springer-Verlag: Berlin, Germany, 2001.
- (3) *Carbon Nanotubes: Properties and Applications*; O'Connell, M. J., Ed.; CRC press/Taylor & Francis: Boca Raton, FL, 2006.
- (4) Saito, R.; Dresselhaus, G.; Dresselhaus, M. S. *Physical Properties of Carbon Nanotubes*; London Imperial College Press: London, 1998.
- (5) Huczko, A. *Appl. Phys. A: Mater. Sci. Process.* **2002**, 74, 617–638.
- (6) Berber, S.; Kwon, Y. K.; Tománek, D. *Phys. Rev. Lett.* **2000**, 84, 4613–4616.
- (7) Hone, J.; Whitney, M.; Piskoti, C.; Zettl, A. *Phys. Rev. B* **1999**, 59, R2514–R2516.
- (8) Hone, J.; Llaguno, M. C.; Nemes, N. M.; Johnson, A. T.; Fischer, J. E.; Walters, D. A.; Casavant, M. J.; Schmidt, J.; Smalley, R. E. *Appl. Phys. Lett.* **2000**, 77, 666–668.
- (9) Mark, H. F.; Othmer, D. F.; Overberger, C. G.; Seaborg, G. T. *Encyclopedia of Chemical Technology*, 3rd ed.; Wiley-Interscience: New York, 1989.
- (10) Hagenmueller, R.; Guthy, C.; Lukes, J. R.; Fisher, J. E.; Winey, K. I. *Macromolecules* **2007**, 40, 2417–2421.
- (11) Andersson, S. P.; Andersson, O. *J. Polym. Sci., Part B: Polym. Phys.* **1998**, 36, 1451–1463.
- (12) Diani, J.; Fayolle, B.; Gilormini, P. *Mol. Simul.* **2008**, 34, 1143–1148.
- (13) Tonpheng, B.; Andersson, O. *Eur. Polym. J.* **2008**, 44, 2865–2873.
- (14) Håkansson, B.; Andersson, P.; Bäckström, G. *Rev. Sci. Instrum.* **1988**, 59, 2269–2275.
- (15) Flory, P. J.; Rehner, J., Jr. *J. Chem. Phys.* **1943**, 11, 512–520.
- (16) Flory, P. J. *J. Chem. Phys.* **1950**, 18, 108–111.
- (17) Orwoll, R. A. *Rubber Chem. Technol.* **1977**, 50, 451–479.
- (18) Tonpheng, B.; Andersson, O. *High Pressure Res.* **2006**, 26, 415–419.
- (19) Tonpheng, B.; Yu, J.; Andersson, O. *High Pressure Res.* **2008**, 28, 587–590.
- (20) Wei, C.; Srivastava, D.; Cho, K. *Nano Lett.* **2002**, 2, 647–650.
- (21) Boochathum, P.; Chiewnawin, S. *Eur. Polym. J.* **2001**, 37, 429–434.
- (22) Nan, C. W.; Liu, G.; Lin, Y.; Li, M. *Appl. Phys. Lett.* **2004**, 85, 3549–3551.
- (23) Huxtable, S.; Cahill, D. G.; Shenogin, S.; Xue, L.; Ozisik, R.; Barone, P.; Usrey, M.; Strano, M. S.; Siddons, G.; Shim, M.; Keblinski, P. *Nat. Mater.* **2003**, 2, 731–734.
- (24) Moniruzzaman, M.; Winey, K. I. *Macromolecules* **2006**, 39, 5194–5205.
- (25) Wunderlich, B. *Thermochim. Acta* **1997**, 300, 43–65.
- (26) Hone, J.; Batlogg, B.; Benes, Z.; Johnson, A. T.; Fischer, J. E. *Science* **2000**, 289, 1730–1733.
- (27) Andersson, O. *Int. J. Thermophys.* **1997**, 18, 195–208.
- (28) Andersson, S. P.; Andersson, O. *Macromolecules* **1998**, 31, 2999–3006.
- (29) Pham, J. Q.; Mitchell, C. A.; Bahr, J. L.; Tour, J. M.; Krishnamoorti, R.; Green, P. F. *J. Polym. Sci., Part B: Polym. Phys.* **2003**, 41, 3339–3345.
- (30) Roland, C. M.; Ngai, K. L.; Plazek, D. J. *Comput. Theor., Polym. Sci.* **1997**, 7, 133–137.
- (31) Adam, G.; Gibbs, J. H. *J. Chem. Phys.* **1965**, 43, 139–146.